

COMPARATOR NETWORK AIDED CHANNEL ESTIMATION AND ACHIEVABLE RATES FOR MIMO RECEIVERS WITH 1-BIT QUANTIZATION

Ana Beatriz L. B. Fernandes and Lukas T. N. Landau

Centre for Telecommunications Studies
Pontifical Catholic University of Rio de Janeiro, Rio de Janeiro, Brazil 22453-900
Email: anafernandes;lukas.landau@cetuc.puc-rio.br

ABSTRACT

The considered low-resolution MIMO receiver implies that the received signals simultaneously are processed by the 1-bit ADCs and the comparator network, where the latter is composed of several simple comparators with binary outputs. In this study, we propose a low-resolution aware linear minimum mean-squared error (LRA-LMMSE) channel estimator for such low-resolution MIMO receivers. By employing the proposed channel estimator and its corresponding estimation error, we build up a lower bound on the ergodic sum rate for the low-resolution aware linear MMSE receiver. Simulation results on the channel estimation match the analytical MSE calculations and it is shown that by taking into account the additional comparator network, the proposed system outperforms the conventional 1-bit MIMO system. Moreover, numerical simulations confirm an advantage in terms of sum rate for the proposed system.

Index Terms— MIMO, 1-bit ADCs, comparator networks, Bussgang theorem, channel estimation, achievable rate

1. INTRODUCTION

An important solution for future cellular networks that scale up in speed and bandwidth is the use of wireless systems with low-precision analog-to-digital converters (ADCs) at the receiver. The power consumption of the ADCs grows exponentially with the number of quantization bits as described in [1]. Therefore, one way to approach a receiver design with low energy consumption is the utilization of 1-bit quantization, which is also favorable in terms of hardware complexity.

Many works have studied large-scale MIMO systems with low resolution ADCs at the front-end. However, the channel estimation is a problem that currently limits the performance of such systems. In this context, the least squares (LS) estimator has been developed in [2]. While a more sophisticated channel estimator is given by the near maximum-likelihood (nML) estimator devised in [3]. Another promising channel estimator is given by the Bussgang Linear Minimum Mean Squared Error (BLMMSE) channel estimator presented in [4], where the authors also derive lower bounds on the theoretical achievable rate for maximum ratio combiner (MRC) and zero-forcing (ZF) receivers.

For signal detection with low-resolution ADCs, different strategies exist in literature, for example iterative detection and decoding (IDD) [5] and sphere decoding [6].

A common used technique in order to mitigate the performance loss caused by the coarse quantization is oversampling. In this regard, the studies in [7–9] considered temporal oversampling at the receiver to achieve better estimation and detection performance.

Another technique to mitigate the performance loss caused by the coarse quantization is given by the utilization of an additional comparator network as presented in [10]. The present paper provides an extension of the study in [10] by devising a linear channel estimation scheme and computing a lower bound on the associated sum rates. Expressions for the low-resolution aware (LRA) linear minimum mean-square-error (LMMSE) channel estimator and the mean-squared error (MSE) of the channel estimate were developed based on the Bussgang decomposition [11], similarly as done in [4, 8]. Numerical results confirm that the consideration of the comparator network is beneficial for channel estimation in terms of MSE. By considering the proposed channel estimator in conjunction with the LRA-MMSE receiver presented in [10], we devise a lower bound on the ergodic sum rate. Numerical results confirm that adding a comparator network to the system increases the sum rate significantly.

The rest of this paper is organized as follows: Section 2 shows the system model and describes the insight of the comparator network. Section 3 derives the linear channel estimator for the proposed system. The lower bound on the sum rate is given in Section 4. In Section 5, the numerical results are presented and Section 6 concludes the study.

Throughout the paper the following notations are used: the bold upper and lower case such as \mathbf{A} and \mathbf{a} denote matrices and vectors, respectively. \mathbf{I}_n is a $n \times n$ identity matrix. The vector or matrix transpose is represented by $(\cdot)^T$. Additionally, $\text{diag}(\mathbf{A})$ is a diagonal matrix only containing the diagonal elements of \mathbf{A} . The inverse of sine function is denoted by $\sin^{-1}(\cdot)$. Moreover, $\text{vec}(\mathbf{A})$ is the vectorized form of \mathbf{A} obtained by stacking its columns, while the inverse of this operation is $\text{unvec}(\mathbf{A})$. Finally, \otimes is the Kronecker product.

2. SYSTEM MODEL

The overall system model is illustrated with blocks in Fig. 1, where the received signal \mathbf{y} for the uplink single-cell MIMO system with N_t single-antenna users and N_r receive antennas is written as

$$\mathbf{y} = \mathbf{H}\mathbf{x} + \mathbf{n}. \quad (1)$$

The vector \mathbf{x} contains complex transmit symbols of the N_t users which have unit power normalization, $\mathbf{H} \in \mathbb{C}^{N_r \times N_t}$ is the channel matrix and $\mathbf{n} \in \mathbb{C}^{N_r \times 1}$ is the noise vector where each element has a variance σ_n^2 . Using the transformation from a complex into a real-valued system, we obtain

$$\begin{bmatrix} \Re\{\mathbf{y}\} \\ \Im\{\mathbf{y}\} \end{bmatrix} = \begin{bmatrix} \Re\{\mathbf{H}\} & -\Im\{\mathbf{H}\} \\ \Im\{\mathbf{H}\} & \Re\{\mathbf{H}\} \end{bmatrix} \begin{bmatrix} \Re\{\mathbf{x}\} \\ \Im\{\mathbf{x}\} \end{bmatrix} + \begin{bmatrix} \Re\{\mathbf{n}\} \\ \Im\{\mathbf{n}\} \end{bmatrix}, \quad (2)$$

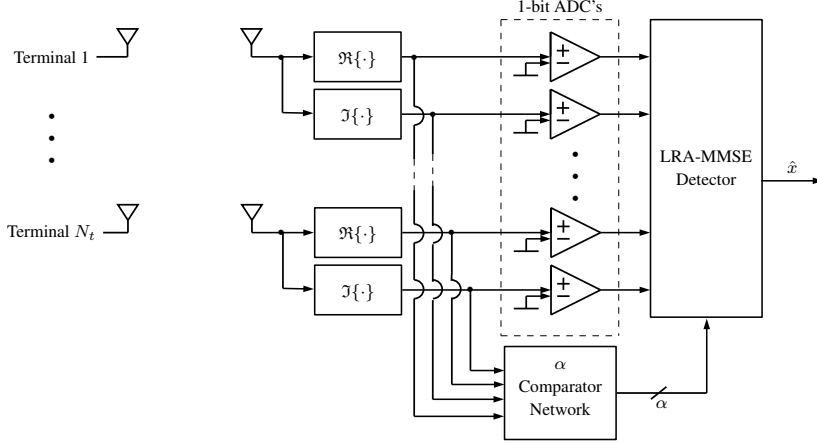


Fig. 1: System model of multi-user MIMO with 1-bit ADCs and an additional comparator network

where $\Re\{\cdot\}$ and $\Im\{\cdot\}$ denote the real and imaginary parts, respectively. A more compact notation for equation (2) reads as

$$\mathbf{y}_R = \mathbf{H}_R \mathbf{x}_R + \mathbf{n}_R. \quad (3)$$

The received signal is then forwarded to the 1-bit ADCs and the comparator network (shown in Fig. 2). Each comparator compares

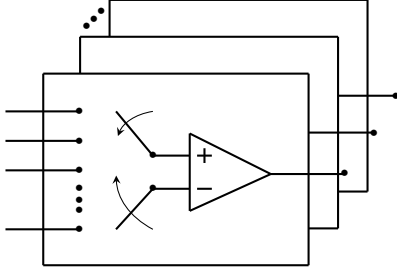


Fig. 2: Insight of the comparator network

two received signals and quantizes the difference as $\{\pm \frac{1}{\sqrt{2}}\}$. Letting $\mathcal{Q}(\cdot)$ represent the 1-bit quantization, the input of the detector is described by

$$\mathbf{z}_Q = \mathcal{Q} \left(\begin{bmatrix} \mathbf{y}_R \\ \mathbf{B}' \mathbf{y}_R \end{bmatrix} \right) = \mathcal{Q} \left(\begin{bmatrix} \mathbf{I}_{2N_r} \\ \mathbf{B}' \end{bmatrix} \mathbf{y}_R \right), \quad (4)$$

where $\mathbf{B}' \in \mathbb{R}^{\alpha \times 2N_r}$ refers to the comparator network and has the form

$$\mathbf{B}' = [\mathbf{B}'_R \quad \mathbf{B}'_I] = \begin{bmatrix} 1 & -1 & 0 & 0 & \cdots & 0 \\ -1 & 0 & 1 & 0 & \cdots & 0 \\ 0 & 0 & 0 & -1 & \cdots & 1 \\ \vdots & \vdots & \vdots & \vdots & \vdots & \vdots \\ 0 & 1 & 0 & 0 & \cdots & -1 \end{bmatrix}. \quad (5)$$

In each row of \mathbf{B}' , there is only one pair of 1 and -1 and the remaining entries are zeros. With $\mathbf{B} = [\mathbf{I}_{2N_r}; \mathbf{B}']$, (4) reads as

$$\mathbf{z}_Q = \mathcal{Q}(\mathbf{z}_R) = \mathcal{Q}(\mathbf{B} \mathbf{y}_R). \quad (6)$$

The novelty of the present study is that 1-bit samples and the comparator output signals, described by $\mathcal{Q}(\mathbf{B}' \mathbf{y}_R)$, are jointly used for the receive processing, like channel estimation.

3. CHANNEL ESTIMATION

In a practical system, the channel state information (CSI) is estimated at the base station (BS) and this knowledge is used to detect the data symbols transmitted by the N_t users. Each transmission block is divided into two sub-blocks: one dedicated to the pilot symbols and the other to the data symbols. The part containing the pilots can be either located at the beginning of each block or spread according to a desired pattern. During the training phase, each terminal simultaneously transmits sequences of τ pilot symbols to the BS, which yields

$$\mathbf{Y}_p = \mathbf{H} \Phi^T + \mathbf{N}_p \quad (7)$$

where $\mathbf{Y}_p \in \mathbb{C}^{N_r \times \tau}$ is the matrix containing the unquantized received signal, $\Phi \in \mathbb{C}^{\tau \times N_t}$ is the matrix of pilot symbols and \mathbf{N}_p is the noise matrix. Vectorizing the received signal yields

$$\text{vec}(\mathbf{Y}_p) = \mathbf{y}_p = \tilde{\Phi} \mathbf{h} + \mathbf{n}_p \quad (8)$$

where $\tilde{\Phi} = (\Phi \otimes \mathbf{I}_{N_r})$, $\mathbf{h} = \text{vec}(\mathbf{H})$ and $\mathbf{n}_p = \text{vec}(\mathbf{N}_p)$. However, due to the addition of the comparator network, we need to work with a real-valued representation of the system. In this case, the received signal \mathbf{y}_{R_p} is defined by

$$\mathbf{y}_{R_p} = \begin{bmatrix} \Re\{\tilde{\Phi}\} & -\Im\{\tilde{\Phi}\} \\ \Im\{\tilde{\Phi}\} & \Re\{\tilde{\Phi}\} \end{bmatrix} \begin{bmatrix} \Re\{\mathbf{h}\} \\ \Im\{\mathbf{h}\} \end{bmatrix} + \begin{bmatrix} \Re\{\mathbf{n}_p\} \\ \Im\{\mathbf{n}_p\} \end{bmatrix} \quad (9)$$

$$= \tilde{\Phi}_R \mathbf{h}_R + \mathbf{n}_{R_p}$$

where $\mathbf{y}_{R_p} \in \mathbb{R}^{\tau(2N_r) \times 1}$ is the real-valued received signal vector. Then, when we multiply equation (9) with an effective comparator network matrix \mathbf{B}_{eff} , we get

$$\mathbf{z}_{R_p} = \mathbf{B}_{\text{eff}} \mathbf{y}_{R_p} = \mathbf{B}_{\text{eff}} \tilde{\Phi}_R \mathbf{h}_R + \mathbf{B}_{\text{eff}} \mathbf{n}_{R_p}, \quad (10)$$

where $\mathbf{B}_{\text{eff}} \in \mathbb{R}^{\tau(2N_r + \alpha) \times \tau(2N_r)}$ is described by

$$\mathbf{B}_{\text{eff}} = \begin{bmatrix} \mathbf{I}_{\tau(2N_r)} \\ \mathbf{B}'_{\text{eff}} \end{bmatrix} = \begin{bmatrix} \mathbf{I}_{\tau(2N_r)} \\ [\mathbf{B}'_{\text{eff}, R} \quad \mathbf{B}'_{\text{eff}, I}] \end{bmatrix}, \quad (11)$$

where $\mathbf{B}'_{\text{eff}, R} = (\mathbf{B}'_R \otimes \mathbf{I}_\tau)$ and $\mathbf{B}'_{\text{eff}, I} = (\mathbf{B}'_I \otimes \mathbf{I}_\tau)$, with \mathbf{B}'_R and \mathbf{B}'_I denoting respectively the parts of the matrix \mathbf{B}' which are associated to the real and imaginary parts of the received signal as shown in (5).

After being processed by the comparators, the quantized signal can be expressed as

$$\mathbf{z}_{\mathcal{Q}_p} = \mathcal{Q}(\mathbf{z}_{R_p}) = \hat{\Phi}_R \mathbf{h}_R + \tilde{\mathbf{n}}_{R_p}, \quad (12)$$

where the right hand side corresponds to a linear model that relies on the Bussgang decomposition approach. In this context, the linear model involves the matrix $\hat{\Phi}_R = \mathbf{A}_p \mathbf{B}_{\text{eff}} \tilde{\Phi}_R$ and the effective noise vector $\tilde{\mathbf{n}}_{R_p} = \mathbf{A}_p \mathbf{B}_{\text{eff}} \mathbf{n}_{R_p} + \mathbf{n}_{q,p}$, with \mathbf{A}_p being a well chosen square matrix and $\mathbf{n}_{q,p}$ being the quantization noise. The Bussgang-based linear operator is chosen independently from \mathbf{z}_{R_p} , in order to minimize the power of the quantization noise as in [12], and is given by

$$\mathbf{A}_p = \mathbf{C}_{\mathbf{z}_{R_p} \mathbf{z}_{\mathcal{Q}_p}}^H \mathbf{C}_{\mathbf{z}_{R_p}}^{-1} = \sqrt{\frac{2}{\pi}} \mathbf{K}, \quad \text{with } \mathbf{K} = \text{diag}(\mathbf{C}_{\mathbf{z}_{R_p}})^{-\frac{1}{2}}, \quad (13)$$

where $\mathbf{C}_{\mathbf{z}_{R_p} \mathbf{z}_{\mathcal{Q}_p}}$ denotes the cross-correlation matrix between the received signal \mathbf{z}_{R_p} and its quantized signal $\mathbf{z}_{\mathcal{Q}_p}$

$$\mathbf{C}_{\mathbf{z}_{R_p} \mathbf{z}_{\mathcal{Q}_p}} = \sqrt{\frac{2}{\pi}} \mathbf{K} \mathbf{C}_{\mathbf{z}_{R_p}} \quad (14)$$

and $\mathbf{C}_{\mathbf{z}_{R_p}} = E\{\mathbf{z}_{R_p} \mathbf{z}_{R_p}^T\}$ denotes the auto-correlation matrix of \mathbf{z}_{R_p}

$$\mathbf{C}_{\mathbf{z}_{R_p}} = \mathbf{B}_{\text{eff}} \tilde{\Phi}_R \mathbf{R}_h \tilde{\Phi}_R^T \mathbf{B}_{\text{eff}}^T + \mathbf{B}_{\text{eff}} \mathbf{C}_{\mathbf{n}_{R_p}} \mathbf{B}_{\text{eff}}^T, \quad (15)$$

where $\mathbf{R}_h = E\{\mathbf{h}_R \mathbf{h}_R^T\}$ and $\mathbf{C}_{\mathbf{n}_{R_p}} = E\{\mathbf{n}_{R_p} \mathbf{n}_{R_p}^T\} = \frac{\sigma_n^2}{2} \mathbf{I}_{\tau(2N_r)}$.

3.1. LRA-LMMSE Channel Estimator

Based on the statistically equivalent linear model in (12), the LRA-LMMSE optimal filter can be obtained through the optimization problem formulated as

$$\begin{aligned} \mathbf{W}_{\text{LMMSE}} &= \arg \min_{\mathbf{W}} E \left[\|\mathbf{h}_R - \mathbf{W} \mathbf{z}_{\mathcal{Q}_p}\|_2^2 \right] \\ &= \mathbf{R}_h \hat{\Phi}_R^T \mathbf{C}_{\mathbf{z}_{\mathcal{Q}_p}}^{-1}, \end{aligned} \quad (16)$$

where the auto-correlation of the quantized signal is calculated as [13]

$$\mathbf{C}_{\mathbf{z}_{\mathcal{Q}_p}} = \frac{2}{\pi} \sin^{-1} \left(\mathbf{K} \Re\{\mathbf{C}_{\mathbf{z}_{R_p}}\} \mathbf{K} \right). \quad (17)$$

The resulting LRA-LMMSE channel estimator corresponds to the linear operation

$$\hat{\mathbf{h}}_{\text{LRA-LMMSE}} = \mathbf{W}_{\text{LMMSE}} \mathbf{z}_{\mathcal{Q}_p} = \mathbf{R}_h \hat{\Phi}_R^T \mathbf{C}_{\mathbf{z}_{\mathcal{Q}_p}}^{-1} \mathbf{z}_{\mathcal{Q}_p} \quad (18)$$

3.2. Mean-Squared Error of the Channel Estimate

The mean-squared error (MSE) of the LRA-LMMSE channel estimate can be expressed as

$$\begin{aligned} \mathcal{M}_{\text{LRA-LMMSE}} &= E \left[\left\| \hat{\mathbf{h}}_{\text{LRA-LMMSE}} - \mathbf{h}_R \right\|_2^2 \right] \\ &= \text{tr} \left(\mathbf{R}_h - \mathbf{R}_h \hat{\Phi}_R^T \mathbf{C}_{\mathbf{z}_{\mathcal{Q}_p}}^{-1} \hat{\Phi}_R \mathbf{R}_h \right), \end{aligned} \quad (19)$$

where it is considered that $E[\tilde{\mathbf{n}}_{R_p} \mathbf{h}_R^T] = \mathbf{0}$.

4. SUM RATE ANALYSIS

4.1. Data Transmission with the utilization of LRA-LMMSE Receiver

It's considered that in the data transmission stage the N_t users simultaneously transmit their data symbols represented by the vector \mathbf{x}_R to the BS, which is a stacked vector with real and imaginary parts. In the present study, real and imaginary parts represent independent data symbols. After processed by the comparators, the quantized signal can be expressed as

$$\begin{aligned} \mathbf{z}_{\mathcal{Q}_d} &= \mathcal{Q}(\mathbf{z}_{R_d}) = \mathcal{Q}(\mathbf{B} \mathbf{y}_{R_d}) \\ &= \mathcal{Q}(\mathbf{B} \mathbf{H}_R \mathbf{x}_R + \mathbf{B} \mathbf{n}_{R_d}) \\ &= \mathbf{A}_d \mathbf{B} \mathbf{H}_R \mathbf{x}_R + \mathbf{A}_d \mathbf{B} \mathbf{n}_{R_d} + \mathbf{n}_{q,d}, \end{aligned} \quad (20)$$

where the same definitions from the previous section apply, but with the subscript p replaced by d , since we changed from the pilots to the data transmission stage. Then, the LRA-LMMSE channel estimate (18) is used to compute a linear receiver which provides an estimate of the data symbols transmitted from the N_t users. In this context, the quantized signal is separated into $2N_t$ streams by multiplying the signal with the receiver filter matrix defined in [10] as $\mathbf{G} = \mathbf{C}_{\mathbf{z}_{\mathcal{Q}_d}}^{-1} \mathbf{C}_{\mathbf{z}_{\mathcal{Q}_d} \mathbf{x}_R}$, which in this case is computed based on the estimated channel. Thereby, we obtain

$$\begin{aligned} \hat{\mathbf{x}}_R &= \mathbf{G} \mathbf{z}_{\mathcal{Q}_d} \\ &= \mathbf{G} \mathbf{A}_d \mathbf{B} (\hat{\mathbf{H}}_R \mathbf{x}_R + \mathcal{E}_R \mathbf{x}_R) + \mathbf{G} \mathbf{A}_d \mathbf{B} \mathbf{n}_{R_d} + \mathbf{G} \mathbf{n}_{q,d}, \end{aligned} \quad (21)$$

where $\hat{\mathbf{H}}_R$ is the estimated channel matrix described by

$$\begin{aligned} \hat{\mathbf{H}}_R &= \begin{bmatrix} \Re\{\hat{\mathbf{H}}\} & -\Im\{\hat{\mathbf{H}}\} \\ \Im\{\hat{\mathbf{H}}\} & \Re\{\hat{\mathbf{H}}\} \end{bmatrix} \quad \text{with } \hat{\mathbf{H}} = \text{unvec}(\hat{\mathbf{h}}) \\ \text{and } \hat{\mathbf{h}} &= [\hat{\mathbf{h}}_{\text{LRA-LMMSE},a} + j\hat{\mathbf{h}}_{\text{LRA-LMMSE},b}], \end{aligned} \quad (22)$$

where $\hat{\mathbf{h}}_{\text{LRA-LMMSE},a}$ corresponds to the first half of $\hat{\mathbf{h}}_{\text{LRA-LMMSE}}$ and $\hat{\mathbf{h}}_{\text{LRA-LMMSE},b}$ to the second. Finally, $\mathcal{E}_R = \mathbf{H}_R - \hat{\mathbf{H}}_R$ is the channel estimation error.

Then, the k th element represents an estimate of the signal of the k th sub-channel, similarly as in [4], with $k \in [1, 2N_t]$, which reads

$$\begin{aligned} \hat{x}_{R_k} &= \underbrace{\mathbf{g}_k \mathbf{A}_d \mathbf{B} \hat{\mathbf{h}}_{R_k} \mathbf{x}_{R_k}}_{\text{desired signal}} + \underbrace{\mathbf{g}_k \sum_{i \neq k} \mathbf{A}_d \mathbf{B} \hat{\mathbf{h}}_{R_i} \mathbf{x}_{R_i}}_{\text{interference}} \\ &\quad + \underbrace{\mathbf{g}_k \sum_{i=1}^K \mathbf{A}_d \mathbf{B} \mathcal{E}_{R_i} \mathbf{x}_{R_i}}_{\text{channel estimation error}} + \underbrace{\mathbf{g}_k \mathbf{A}_d \mathbf{B} \mathbf{n}_{R_d}}_{\text{AWGN noise}} + \underbrace{\mathbf{g}_k \mathbf{n}_{q,d}}_{\text{quant. noise}}, \end{aligned} \quad (23)$$

where \mathbf{g}_k and $\hat{\mathbf{h}}_{R_k}$ are the k th columns of the matrices \mathbf{G}^T and $\hat{\mathbf{H}}_R$, respectively. Moreover, \mathcal{E}_{R_i} is the i th column of the matrix \mathcal{E}_R .

4.2. Lower bounding the Sum Rate

Since the Gaussian noise case corresponds to the worst case scenario, we can find a lower bound for the achievable rate by interpret the quantization noise as Gaussian, with an equivalent noise covariance matrix [12]. In this regard, the equivalent noise covariance matrix is given by

$$\begin{aligned} \mathbf{C}_{\mathbf{n}_{q,d}} &= E \left[(\mathbf{z}_{\mathcal{Q}_d} - \mathbf{A}_d \mathbf{z}_{R_d})(\mathbf{z}_{\mathcal{Q}_d} - \mathbf{A}_d \mathbf{z}_{R_d})^T \right] \\ &= \mathbf{C}_{\mathbf{z}_{\mathcal{Q}_d}} - \mathbf{A}_d \mathbf{C}_{\mathbf{z}_{R_d}} \mathbf{A}_d^T, \end{aligned} \quad (24)$$

$$I_{R_k} = E \left[\frac{1}{2} \log_2 \left(1 + \frac{|\mathbf{d}_k \hat{\mathbf{h}}_{R_k}|^2}{\sum_{i \neq k}^K |\mathbf{d}_k \hat{\mathbf{h}}_{R_i}|^2 + \sum_{i=1}^K |\mathbf{d}_k \epsilon_{R_i}|^2 + \sigma_n^2 \|\mathbf{d}_k\|_2^2 + 2\mathbf{g}_k \mathbf{C}_{n_{q,d}} \mathbf{g}_k^T} \right) \right] \quad (25)$$

where $\mathbf{d}_k = \mathbf{g}_k \mathbf{A}_d \mathbf{B}$.

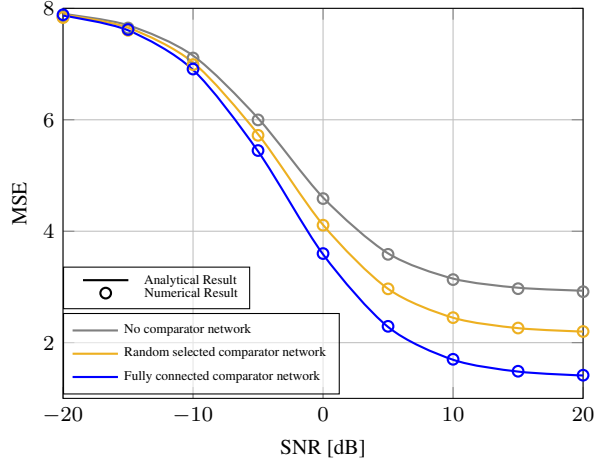


Fig. 3: MSE comparisons of LRA-LMMSE channel estimators with and without comparator network in 2×4 MIMO systems.

where $\mathbf{C}_{z_{Q_d}} = E[\mathbf{z}_{Q_d} \mathbf{z}_{Q_d}^T]$ is the auto-correlation matrix of the quantized data signal, like in (17), and $\mathbf{C}_{z_{R_d}} = E[\mathbf{z}_{R_d} \mathbf{z}_{R_d}^T] = \frac{1}{2} \mathbf{B} \mathbf{H}_R \mathbf{H}_R^T \mathbf{B}^T + \frac{\sigma_n^2}{2} \mathbf{B} \mathbf{B}^T$ is the auto-correlation matrix of the received data signal.

Using this approach, the ergodic achievable rate per sub-channel is lower bounded by (25), where the expectation operator is taken with respect to channel realizations and channel estimation realizations. According to prior literature [12], this method provides an accurate lower bound especially for the low SNR regime. Finally, the sum rate is lower-bounded by $\sum_{k=1}^K I_{R_k}$.

5. NUMERICAL RESULTS

In this section, an uplink single-cell 1-bit MIMO system with $N_t = 2$ and $N_r = 4$ is considered. The pilot sequences are column-wise orthogonal with length $\tau = N_t$, i.e., $\Phi^T \Phi = \tau \mathbf{I}_{N_t}$. The SNR is defined as $10 \log(\frac{1}{\sigma_n^2})$, which is the average receive SNR per user per antenna. The MSE performance plots are obtained by taking the average of 4000 different channels and 4000 noise realizations per channel.

The MSE comparison between the LRA-LMMSE channel estimators with fully and partially connected comparator networks are shown in Fig. 3, where partially connected refers to comparator networks of $2N_r$ comparators with input signals from each two random antennas in terms of real or imaginary parts. The case of fully connected networks refers to comparator networks where all possible combinations are considered. The lines labeled with ‘‘Analytical Result’’ are obtained with (19) while the marks labeled with ‘‘Numerical Result’’ are obtained with the MSE of the simulated channel estimator in (18). The presented numerical and analytical results are

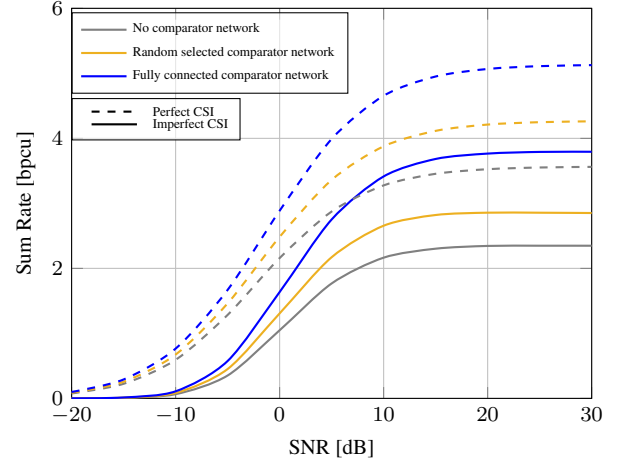


Fig. 4: Sum Rate comparisons of LRA-LMMSE channel estimators with and without comparator network in 2×4 MIMO systems.

aligned, which confirms the accuracy of the proposed model. As expected, the system with the fully connected method achieves the best MSE performance. However, it can be seen that the approach with the comparator network using random selected inputs is also beneficial in terms of MSE in comparison to the case without comparator network.

In the second experiment, we compare the lower bound of the ergodic sum rate with and without a random selected comparator network with $2N_r$ comparators. The sum rate versus SNR is shown in Fig. 4, which indicates a significant benefit for the system that utilizes the additional comparator network. Note that the increased sum rate is not only due to a more accurate channel estimation but also due to the comparator network aided receive processing.

6. CONCLUSIONS

In this study, the LRA-LMMSE channel estimator and corresponding sum rates for the comparator network aided 1-bit MIMO systems are proposed. The numerical simulations match with the corresponding analytical channel estimation performance in terms of the MSE. By considering that the base station employs a linear receiver and using the proposed channel estimate and the corresponding estimation error, we have derived an expression for lower bounding the ergodic sum rate. Simulation results show that the proposed comparator network based system outperforms the conventional 1-bit receiver in terms of channel estimation and sum rates.

ACKNOWLEDGMENT

This work has been supported by the ELIOT ANR18-CE40-0030 and FAPESP 2018/12579-7 project.

7. REFERENCES

- [1] R. H. Walden, "Analog-to-digital converter survey and analysis," *IEEE J. Sel. Areas Commun.*, vol. 17, no. 4, pp. 539–550, Apr. 1999.
- [2] C. Risi, D. Persson, and E. G. Larsson, "Massive MIMO with 1-bit ADC," *arXiv preprint arXiv:1404.7736*, 2014.
- [3] J. Choi, J. Mo, and R. W. Heath, "Near Maximum-Likelihood Detector and Channel Estimator for Uplink Multiuser Massive MIMO Systems with One-Bit ADCs," *IEEE Transactions on Communications*, vol. 64, no. 5, pp. 2005–2018, 2016.
- [4] Y. Li, C. Tao, G. Seco-Granados, A. Mezghani, A. L. Swindlehurst, and L. Liu, "Channel Estimation and Performance Analysis of One-Bit Massive MIMO Systems," *IEEE Transactions on Signal Processing*, vol. 65, no. 15, pp. 4075–4089, Aug. 2017.
- [5] Z. Shao, R. C. de Lamare, and L. T. N. Landau, "Iterative Detection and Decoding for Large-Scale Multiple-Antenna Systems With 1-Bit ADCs," *IEEE Wireless Commun. Lett.*, vol. 7, no. 3, pp. 476–479, Jun. 2018.
- [6] Y. Jeon, N. Lee, S. Hong, and R. W. Heath, "One-Bit Sphere Decoding for Uplink Massive MIMO Systems With One-Bit ADCs," *IEEE Trans. Wireless Commun.*, vol. 17, no. 7, pp. 4509–4521, Jul. 2018.
- [7] Z. Shao, L. T. N. Landau, and R. C. de Lamare, "Sliding Window Based Linear Signal Detection Using 1-Bit Quantization and Oversampling for Large-Scale Multiple-Antenna Systems," in *2018 IEEE Statistical Signal Processing Workshop (SSP)*, Freiburg, Germany, Jun. 2018, pp. 183–187.
- [8] Z. Shao, L. T. N. Landau, and R. C. de Lamare, "Channel Estimation for Large-Scale Multiple-Antenna Systems Using 1-Bit ADCs and Oversampling," *IEEE Access*, vol. 8, pp. 85243–85256, 2020.
- [9] Z. Shao, L. T. N. Landau, and R. C. de Lamare, "Dynamic Oversampling for 1-Bit ADCs in Large-Scale Multiple-Antenna Systems," *IEEE Transactions on Communications*, 2021.
- [10] A. B. L. B. Fernandes, Z. Shao, L. T. N. Landau, and R. C. de Lamare, "Comparator Network Aided Detection for MIMO Receivers with 1-bit Quantization," in *Proc. Asilomar Conference on Signals, Systems and Computers*, Pacific Grove, CA, USA, Nov 2020.
- [11] J. J. Bussgang, "Crosscorrelation functions of amplitude-distorted Gaussian signals," *Res. Lab. Elec., MIT*, vol. Tech. Rep. 216, Mar. 1952.
- [12] A. Mezghani and J.A. Nossek, "Capacity Lower Bound of MIMO Channels with Output Quantization and Correlated Noise," in *2012 International Symposium on Information Theory*, Cambridge, MA, Jul. 2012.
- [13] G. Jacovitti and A. Neri, "Estimation of the autocorrelation function of complex Gaussian stationary processes by amplitude clipped signals," *IEEE Transactions on Information Theory*, vol. 40, no. 1, pp. 239–245, Jan. 1994.